Application of a collisional radiative model to atomic hydrogen for diagnostic purposes

D. Wünderlich [a] S. Dietrich [b] U. Fantz [a]

[a] *Max-Planck-Institut für Plasmaphysik, EURATOM Association, Boltzmannstr. 2, D-85748 Garching, Germany*

[b] *Lehrstuhl für Experimentelle Plasmaphysik, Universität Augsburg, Universitätsstr. 1, D-86135 Augsburg, Germany*

Abstract

Optical emission spectroscopy is one of the standard diagnostic methods to determine plasma parameters. In hydrogen plasmas often the intensity of the Balmer lines is recorded. To analyze such measurements population models for the hydrogen atom are needed. The flexible package `Yacora` is used to construct a new collisional radiative model for low pressure, low temperature hydrogen plasmas. This model includes six possible excitation channels: effective excitation of H, recombination of H^+, dissociative excitation of H_2, dissociative recombination of H_2^+, dissociative recombination of H_3^+ and mutual neutralization of H^- and H_x^+. The model is applied to an uniform ECR plasma with high dissociation degree and low ionization degree, i.e. electron collision excitation from H is the dominant excitation channel. The cross sections for this channel taken from literature showed a non-physical discontinuity at electron energies close to the threshold energy. This discontinuity has been removed by using a smoothing procedure. For known plasma parameters the deviation between measured and calculated population densities decreases significantly by using the smoothed data. Furthermore the agreement of the electron density deduced from the ratio H_β/H_γ with results of other diagnostic methods is enhanced dramatically.

Key words: Hydrogen atom, Low temperature, low pressure plasma, Collisional radiative model, Optical emission spectroscopy, Electron collision excitation, Line ratio method
PACS: 52.65.-y, 52.70.-m, 32.30.-r, 52.20.Fs

Email address: `dirk.wuenderlich@ipp.mpg.de` (D. Wünderlich).

1 Introduction

Low pressure, low temperature plasmas are used in a wide range of technical and research applications [1]. Most of these plasmas contain a certain amount of hydrogen atoms produced by dissociation of H_2 or other molecules, e.g. hydrocarbons or silanes.

The most important plasma parameters in these plasmas are temperature, density and velocity distribution functions of the particles. Plasma diagnostics which determines the plasma parameters is a key issue to improve the understanding of plasma processes [2,3].

Plasma diagnostics usually is based on the measurement of externally accessible physical parameters of the plasma. For example a spectrometer can be used to record the intensity of a radiative transition. Models in which the plasma parameters are used as free parameters are applied to predict values of the measured parameter. A comparison of the results of measurement and calculation enables the determination of the plasma parameters.

For low pressure, low temperature plasmas, many different diagnostic methods are available [2,3]. One of these methods is the optical emission spectroscopy (OES) [4–6], which is based on a very simple and robust experimental set-up. One main advantage of this method is its non-invasive nature, i.e. the plasma is not affected by the measurements.

For the interpretation of spectrosopically measured intensities population models are needed. Such models calculate population densities of excited states in atoms, molecules or ions depending on the plasma parameters. For very high electron densities ($n_e \gtrsim 10^{24}$ m^{-3} in hydrogen plasmas) the states thermalize and the local thermodynamic equilibrium (LTE) can be applied. For very low electron densities ($n_e \lesssim 10^{17}$ m^{-3} in hydrogen plasmas) the corona equilibrium which balances electron collision excitation from the ground state with radiative transitions is valid. For intermediate electron densities the excitation and de-excitation processes for all states in the atom, molecule or ion have to be balanced by the population model [7]. Such models are called collisional radiative (CR) models [8–10]. For high and low electron densities CR models represent the LTE and corona equilibrium, respectively.

The first CR model for H was developed by Johnson and Hinnov [11]. Since then other CR models for the hydrogen atom have been presented [12,13], the most prominent one is the `ADAS` package [13]. The typical application ranges of these models are recombining ($T_e < 1$ eV) or ionizing plasmas ($T_e > 10$ eV) which means that the population densities of exited states are determined mainly by recombination from H^+ and electron collision excitation from H, respectively.

In typical process plasmas [14] and sources for positive [15] or negative hydrogen ions [16] the electron temperature is between these values. In this intermediate parameter range population processes from additional neutral particles (H_2) or ions (H_2^+, H^-) can have an influence on the population of excited states. Additionally, the average energy of the plasma particles is either below or close to the threshold energy of some of the excitation processes. Thus, the corresponding cross sections and the energy distribution functions of the involved particles have to be known very accurately for low energies.

The flexible package `Yacora` was developed and used to construct a new CR model for hydrogen plasmas. This paper describes in more detail the application of the model to an uniform ECR plasma with electron temperatures in the parameter range between recombining and ionizing plasmas ($1\ \mathrm{eV} < T_e < 10\ \mathrm{eV}$), high dissociation degree and low ionization degree, i.e. electron collision excitation from H is the dominant excitation channel. This regime is outside the parameter ranges in which the previously existing CR models for H have been tested. Comparison of measured and calculated population densities enables the revision of the cross sections available in literature for collision excitation from the ground state of H at electron energies close to the threshold.

2 Physics of collisional radiative models

When an excited state p in an atom, molecule or ion is de-excited by a radiative transition to an energetically lower-lying state q, the intensity of the emitted radiation can be expressed by the line emission coefficient ε_{pq}.

$$\varepsilon_{pq} = n_p A_{pq} \frac{h\nu}{4\pi}, \tag{1}$$

where n_p is the population density of p, A_{pq} the transition probability and ν the frequency of the transition. If the transition probability and frequency are known, the population density can be deduced from a measured value of the line emission coefficient:

$$n_p = \frac{\varepsilon_{pq}}{A_{pq}} \frac{4\pi}{h\nu}. \tag{2}$$

The population density depends on the plasma parameters such as T_e and n_e and can be calculated by CR models. To ease such calculations, often the fact is utilized that the different processes which are dominant for reaching the equilibrium population of the species or states present in the plasma have different time scales. In low pressure, low temperature plasmas the population density

of excited states is mainly determined by collisions with electrons or heavy particles and radiation. The ground state population of atoms, molecules and ions mainly depends on transport processes [17]. The population density of excited states is established on a time scale of nanoseconds while the ground state densities change much more slowly (typically on a timescale between milliseconds and microseconds). Thus, the ground state densities can be considered as quasi-constant input values for CR models. Exact knowledge of the different time scales allows for considering even the population densities of some excited states (e.g. metastable states or vibrational levels of a molecular ground state) as quasi-constant [17].

The temporal dependency of the population density n_p can be described by a rate equation:

$$\frac{\mathrm{d}n_p}{\mathrm{d}t} = \sum_{q>p} A_{qp} n_q - \sum_{q<p} A_{pq} n_p + \\ + n_\mathrm{e} \left(\sum_{q \neq p} X_{qp} n_q - \sum_{q \neq p} X_{pq} n_p + (\alpha + \beta n_\mathrm{e}) n_+ - S_p n_p \right) , \tag{3}$$

where A_{qp} and A_{pq} are the transition probabilities for spontaneous emission from q to p and p to q, respectively. X_{qp} and X_{pq} are the rate coefficients for excitation or de-excitation by electron collisions. α and β are the rate coefficients for recombination of an ion with density n_+ and S_p is the rate coefficient for ionization of the state p. Equation (3) must be extended when heavy particle collisions (for example Penning ionization and quenching), self-absorption due to optical thickness of emission lines [18] or other additional processes have to be considered.

Such equations can be assembled for all excited states, resulting in a system of coupled ordinary differential equations. If the equation system is linear, the steady state population densities (right hand side of the equation system yields zero) can be calculated easily by inverting a matrix. Otherwise the solution has to be determined by integrating the equations beginning with a specified starting condition. In both cases the solution of equation (3) can be expressed in terms of so-called population coefficients R_{0p} [12]:

$$R_{0p} = \frac{n_p}{n_\mathrm{e} \cdot n_0}, \tag{4}$$

where n_0 denotes the density of the ground state or another species with quasi-constant density. It can be seen from equation (4) that population coefficients primarily depend on the electron density and the ground state density. The density n_p calculated by the CR model depends on electron temperature and

electron density. Further dependencies of n_p arise for extended forms of equation (3). When for example heavy particle collisions are considered, density and temperature of the involved particles are additional parameters.

The population density of interest can be determined by a simple transformation of equation (4):

$$n_p = R_{0p} \cdot n_\mathrm{e} \cdot n_0. \tag{5}$$

If the population density n_p depends on more than one species S with quasi-constant density, additional coupling processes have to be considered by calculating population coefficients for each of these species. Then n_p is the result of a summation:

$$n_p = n_\mathrm{e} \cdot \sum_S R_{Sp} \cdot n_S, \tag{6}$$

where R_{Sp} are the population coefficients for coupling of the different species S to the excited states and n_S the ground state densities of these species.

For constructing CR models for atoms, the probabilities of several thousand reactions have to be known in form of cross sections, rate coefficients or transition probabilities. The complexity increases dramatically if vibrationally and rotationally excited states of molecules have to be considered. When the probability for a certain reaction is not known, often the value is deduced by assumptions or extrapolations, e.g. from the known probability of a similar reaction [19]. One example for this approach is the detailed balance which is quite commonly used to deduce the probability for a reverse reaction from the known probability of the forward reaction.

The accuracy of the results calculated by the model strongly depends on the accuracy of the input data. Thus, a critical check of the input data is essential.

3 The collisional radiative model for the hydrogen atom

3.1 Fundamental characteristics of the collisional radiative model for H

Hydrogen represents the simplest atom. It consists of a number of electronically excited states which are degenerate due to different possible orientations of angular momentum and spin of the valence electron. In case of non-existing strong external fields, the energetic splitting of the degenerate states can be neglected. Due to strong coupling processes with non-metastable states of the

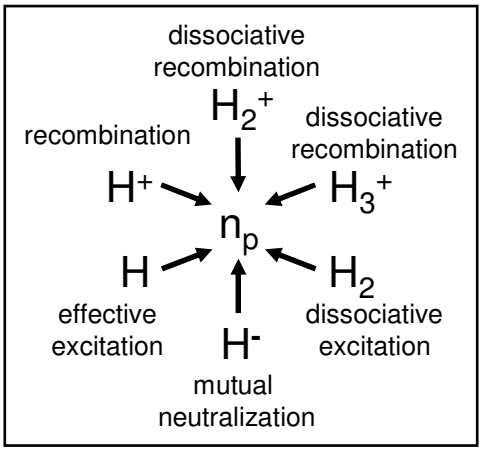

Fig. 1. In low pressure, low temperature plasmas the population density of an excited state in the hydrogen atom can be coupled to six species with quasi-constant density.

same main quantum number, the metastable sub-state 2s is not needed to be considered explicitly [20]. Thus, for the hydrogen atom it is sufficient to resolve just the main quantum number in CR models.

In principle, in low pressure, low temperature hydrogen plasmas the population densities of the excited states of the hydrogen atom are coupled to six different species with quasi-constant density. The coupling processes are shown schematically in figure (1). The equilibrium population density n_p is calculated by equation (6), considering these coupling channels:

$$n_p = n_\mathrm{e} \left(R_{\mathrm{H}p} n_\mathrm{H} + R_{\mathrm{H}^+p} n_{\mathrm{H}^+} + R_{\mathrm{H}_2p} n_{\mathrm{H}_2} + R_{\mathrm{H}_2^+p} n_{\mathrm{H}_2^+} + R_{\mathrm{H}_3^+p} n_{\mathrm{H}_3^+} + R_{\mathrm{H}^-p} n_{\mathrm{H}^-} \right) \quad (7)$$

The terms in parentheses denote effective excitation of H, recombination of H^+, dissociative excitation of H_2, dissociative recombination of H_2^+, dissociative recombination of H_3^+ and mutual neutralization of H^- and H_x^+, respectively.

One requirement to the flexible package `Yacora` was the ability to handle non-linear processes, for example the self-absorption due to optical thickness of emission lines. The solution of equation system (3) has to be determined by an integration technique. Because of the stiffness of the equation system, ordinary integration techniques as for example the Runge Kutta method [21] are too slow and the solver `CVODE` [22] was chosen instead.

`Yacora` allows the user to easily define the names of all species and states, the probabilities for all reactions and the initial conditions. The probabilities of collision processes can be given either as rate coefficients or cross sections. In the latter case additionally an electron energy distribution function has to be defined. This offers the possibility to perform calculations for plasma regimes with non-Maxwellian EEDF which are often observed in low pressure, low

temperature plasmas [23].

The CR model for the hydrogen atom includes the 40 energetically lowest lying electronic states of the atom (H(1) ... H(40)). Table 1 gives an overview of all reactions included in the model and the underlying input data. The total number of reactions included in the CR model is 2359.

The input files use the most recent data available in literature. As far as possible cross sections instead of rate coefficients were used for defining the reaction probabilities.

The reactions included to the model are mainly electron collision processes and radiation. The only heavy particle collision considered is the mutual neutralization of H^- and H_x^+. When the negative ion density is sufficient, this reaction can have a significant influence on the population density of the excited state H(3) and thus on the emission of the Balmer line H_α [24]. Instead of implementing the single mutual neutralization processes of H^- with H^+, H_2^+ and H_3^+, a cumulative cross section is used. Other excitation or ionization processes by collisions with heavy particles can be neglected due to the small average energy of the heavy particles (typically a few hundred Kelvin) in the plasmas investigated.

Dissociative recombination of H_3^+ can occur via two different reaction channels. Reaction products are either three hydrogen atoms in their ground state H(1) or a hydrogen molecule and an excited atom. The total cross section and the branching ratio of the two channels have been investigated extensively by means of calculations and measurements [25]. The quantum state distribution of the atom produced by the second channel is not exactly known [26], but it can be deduced from calculations of electronically excited states of H_3 that for electron energies above 1 eV the dominant reaction product is H(2) [27]. Thus, the cross section and branching ratio measured in a storage ring [28] were implemented to the CR model, assuming that the second channel always produces an atom in the state H(2).

Due to its quasi-constant character, the density of the ground state H(1) is used as fixed parameter for the solution process. Thus, reactions which only change the ground state density and not the population densities of exited states does not need to be considered by the model. An example of this would be the stripping of negative ions by electrons: $H^- + e^- \rightarrow H(1) + 2e^-$.

Although the hydrogen atom is the simplest atom, for some reactions no cross sections or rate coefficients are available in literature. In this case the same estimations as done in [12] are used.

The rate coefficients for de-excitation by electron collisions are calculated by applying the detailed balance to the excitation rate coefficients. The influ-

Table 1
Overview of the reactions included in the CR model for the hydrogen atom.

Process	Reaction	Reference
Excitation by e^- collision	$H(q) + e^- \rightarrow H(p > q) + e^-$	[26]
De-excitation be e^- collision	$H(q) + e^- \rightarrow H(p < q) + e^-$	[26] (see text)
Spontaneous Emission	$H(q) \rightarrow H(p < q) + h\nu$	[18,29] (see text)
Ionization	$H(q) + e^- \rightarrow H^+ + 2e^-$	[26]
Recombination of H^+	$H^+ + 2e^- \rightarrow H(p) + e^-$	[12]
	$H^+ + e^- \rightarrow H(p) + h\nu$	[12]
Dissociation of H_2	$H_2 + e^- \rightarrow H(p) + H(1) + e^-$	[12]
Dissociation of H_2^+	$H_2^+ + e^- \rightarrow H(p) + H^+ + e^-$	[12]
Dissociative recombination of H_2^+	$H_2^+ + e^- \rightarrow H(p) + H(1)$	[12]
Dissociative recombination of H_3^+	$H_3^+ + e^- \rightarrow H(p) + H_2$	[28] (see text)
Mutual neutralization ($x = 1 \ldots 3$)	$H_x^+ + H^- \rightarrow H(p) + H(1)$	[30]

ence of self-absorption due to the optical thickness of the Lyman lines on the population densities of excited states is taken into account by multiplying the transition probabilities for spontaneous emission with the appropriate population escape factors as suggested in [18].

For coupling of the population densities only to the hydrogen atom the results of the model are in excellent agreement with the results of the CR models described in [12,13]. In a next step a critical investigation on the cross sections for the excitation channel from the ground state H(1) at low electron temperatures is carried out.

3.2 Recent improvement of the input data for atomic hydrogen

The cross sections for excitation from the ground state H(1) to excited states H(p) of the atom by electron collision excitation were taken from the latest available compilation [26] and are shown in figure 2 for $p = 2 \ldots 7$ and electron energies up to $E_e = 100$ eV.

For high electron energies ($E_e \gtrsim 80$ eV) the cross sections show a steady decrease with increasing quantum number. For electron energies near the threshold a discontinuity appears between the cross sections for the excitation processes H(1) $\rightarrow$ H(5) and H(1) $\rightarrow$ H(6). From the physics point of view this discontinuity is not explainable since the only difference between the two states H(5) and H(6) is their slightly different energy (13.06 eV compared to

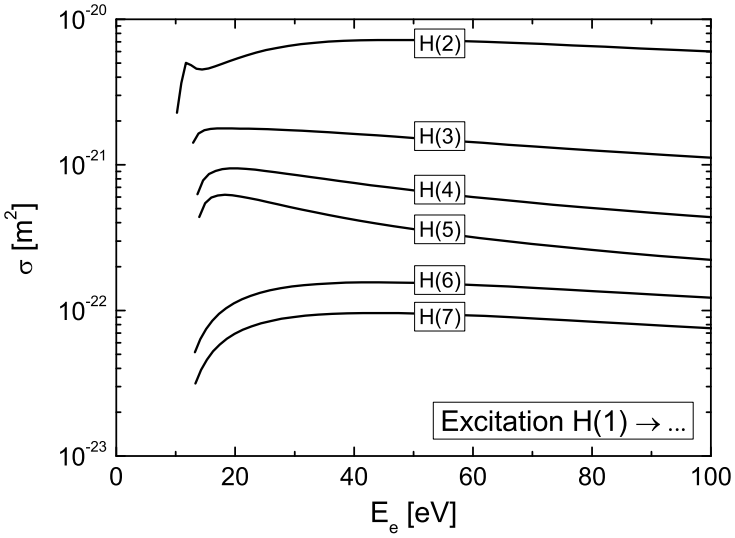

Fig. 2. Cross sections from [26] for the excitation of the six energetically lowest lying excited states of H from the ground state H(1). For low electron energies a discontinuity appears between the cross sections for H(1) → H(5) and H(1) → H(6).

13.23 eV). Since the discontinuity is located at low energies, it will have a significant impact on interpretation of low temperature plasmas based on CR model calculations.

The report [26] represents the most recent available compilation of cross sections from other sources. The discontinuity observed is due to the junction between data taken from two different primary data sources. The cross sections for excitation of lower quantum numbers $(\mathrm{H}(p), p \leq 5)$ for low electron energies ($\mathrm{E_e} \lesssim 50\,\mathrm{eV}$) are a composition of several calculations, amongst them the R-Matrix method. For higher quantum numbers $(\mathrm{H}(p), p \geq 6)$ a semi-empirical modification of the Born-Bethe formula has been used [31].

Although, in principle the R-Matrix method is very accurate, the convergence of R-Matrix calculations is slow when the number of basis set eigenfunctions needed to construct the excited state is large [32]. The number of needed eigenfunctions increases strongly with the main quantum number of the excited state. For too low numbers of considered eigenfunctions the accuracy of the results is poor. For Li this problem was resolved by including a larger set of bound and continuum basis set eigenfunctions [32]. Up to now no similar calculations were performed for the hydrogen atom. At the time when the R-Matrix calculations included in [26] were performed, computation of the cross sections for excitation of H(5) was close to the limit of what is technically possible. The only available more recent data [33] is given in form of rate coefficients and has been calculated assuming a Maxwellian EEDF. Using these rate coefficients does reduce the observed discontinuity but not remove it completely. Thus, it has been concluded that the existing cross sections and rate coefficients for excitation of H(5) are rather inaccurate [34].

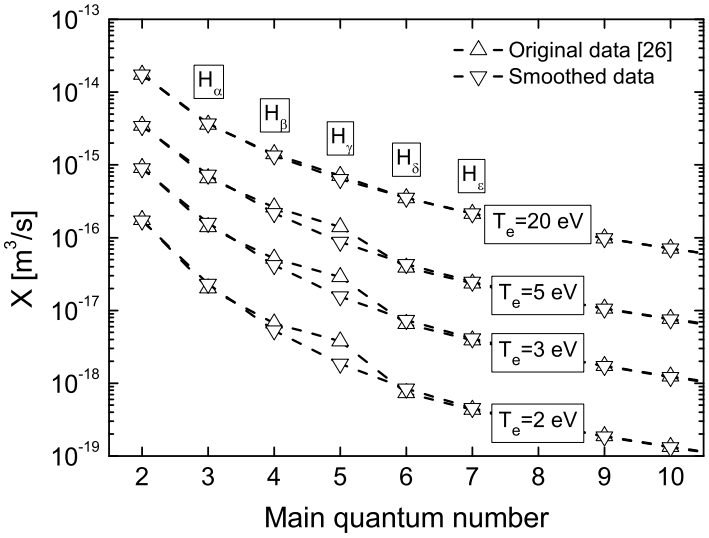

Fig. 3. Rate coefficients for the electron collision excitation of several states of H from the ground state H(1) at selected values of the electron temperature. The data taken from [26] is compared with the result of the fit performed.

For the excitation of higher quantum numbers $(\mathrm{H}(p), p \geq 6)$ the cross sections calculated using the semi-empirical modification of the Born-Bethe formula [31] are the only complete data set available in literature. In [35] it is shown that for high electron energies these cross sections correctly reproduce Born-exchange calculations for $p = 6, 7$ and Born-Rudge calculations for $p = 10$.

As proposed solution, smoothly combining the R-Matrix rate coefficients for excitation of $(\mathrm{H}(p), p \leq 4)$ taken from [33] with rate coefficients based on the semi-empirical cross sections for $(\mathrm{H}(p), p \geq 6)$ will result in the most accurate data set possible in the moment. To do so, the latter rate coefficients were calculated using a Maxwellian EEDF. For 100 electron temperatures in the range $\mathrm{T_e} = 0.5 \ldots 25.0$ eV the different rate coefficients were plotted over the main quantum number. To obtain a smoothed input data set for the collisional radiative model a fit was performed. For four temperatures and the ten energetically lowest lying electronic states the resulting rate coefficients are shown in figure 3.

Also shown in figure 3 are the non-smoothed rate coefficients. It can be seen that the discontinuity at $\mathrm{H}(1) \rightarrow \mathrm{H}(5)$ is particularly pronounced for low electron temperatures, which is a direct result of the shape of the cross sections shown in figure 2. For higher electron temperatures the discontinuity is less pronounced and for $\mathrm{T_e} > 20\,\mathrm{eV}$ it vanishes almost completely. This explains why the discontinuity was not detected previously by other CR models for ionizing plasmas since these models are applied typically to plasmas with

$T_e \gtrsim 10\,eV$.

The deviation between the original data and the fit performed is a factor 2 for H(5) and $T_e = 2\,eV$ and decreases with increasing electron temperature. For lower and higher quantum numbers the fit represents the original data. This means that for cold plasmas in which the direct excitation from H dominates, the radiation of H_γ is overestimated by a factor 2 when the non-smoothed data is used.

To investigate the consequences of this overestimation, population densities calculated with the CR model using both the original and the smoothed input data are compared with experimental results.

4 The experiment

Spectroscopic measurements on a low pressure, low temperature plasma with known plasma parameters were performed. Since measurements by OES average the emitted intensity over a specific line-of-sight, the measurements were performed on an uniform and stationary ECR plasma.

The ECR reactor used to generate the plasma is shown schematically in figure 4. The experiment consists of a cylindrical vacuum vessel ($d = 15\,cm$, $h = 31\,cm$). The top and bottom of this cylinder are closed by a quartz plate and an aluminum plate, respectively. The reactor is evacuated to the background pressure $5 \cdot 10^{-6}\,mbar$ by a pumping system consisting of a turbo molecular pump and a forepump. Different gas mixtures can be filled into the vessel by means of three calibrated mass flow meters.

The microwave with a frequency of 2.45 GHz is generated by a magnetron ($P_{max.} = 1\,kW$) and transferred into the plasma by a rectangular waveguide. This frequency corresponds to the electron cyclotron resonance (ECR) frequency at a magnetic field strength of 87.5 mT. Since the microwave is introduced from the high-field-side of the magnetic field, a good coupling of the microwave power into the plasma is achieved [36,37]. A set of electromagnetic Helmholtz coils ($I_{max.} = 50\,A$) are used to generate a homogeneous magnetic field of 87.5 mT in a large volume inside the chamber which ensures a good plasma uniformity.

The experiment can be operated in a wide range of pressure and microwave power ($p = 0.01 - 20\,Pa$, $P = 30 - 1000\,W$) for different gas mixtures. Thus, a wide range of plasma parameters is accessible ($T_e = 1 - 12\,eV$, $n_e = 10^{16} - 5 \cdot 10^{18}\,m^{-3}$). From the emission of H_β and the molecular Fulcher band it can be deduced [6] that the dissociation degree inside the source typically is high

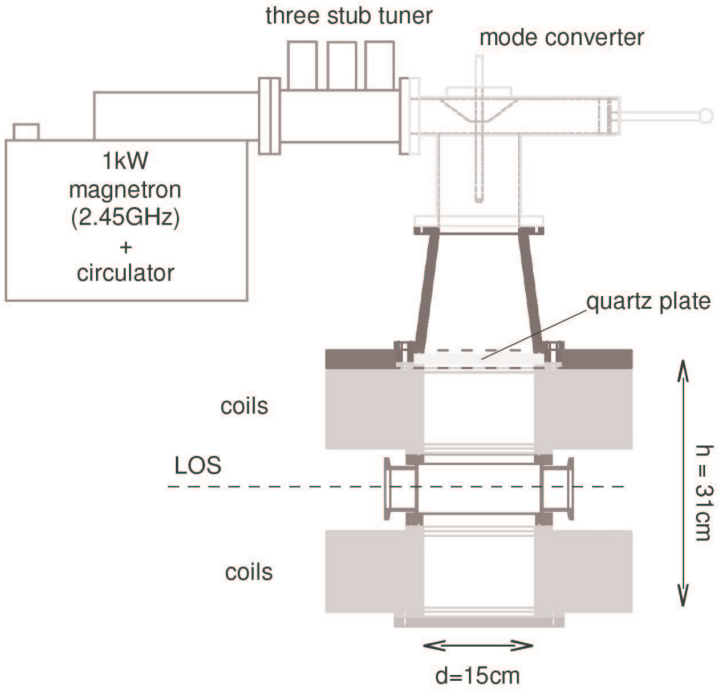

Fig. 4. Schematic overview of the ECR reactor used to generate an uniform hydrogen plasma.

(H/H_2 density ratio $\gtrsim 0.05$). Langmuir probe measurements show that the ionization degree is low (ratio $n_e/n_0 = 10^{-5} - 10^{-3}$).

Between the two magnetic coils the vacuum vessel is equipped with large diagnostic ports. These ports enable access of diagnostic systems (OES, electrical probes: Langmuir probe and double probe, microwave interferometry) to the plasma. For measuring line emissivities, a spectroscopic system is used, consisting of a Czerny Turner spectrometer (f = 750 mm, 1800 G/mm grating) which is connected with the plasma source by a fibre optics system. The light is detected by a 2500×600 pixel CCD detector. The spectroscopic system was absolutely calibrated in the range 200-900 nm by means of an Ulbricht sphere and a D_2 lamp.

5 Results

For investigating the influence of the smoothing procedure described in section 3.2, the CR model was applied to the experiment described in section 4. Plasmas containing 10 % hydrogen, 5 % argon and 85 % helium were generated at 0.5, 4, 10 and 15 Pa pressure.

Using Langmuir probe and double probe measurements it was shown that the spatial profile of the electron density inside the experiment is almost flat

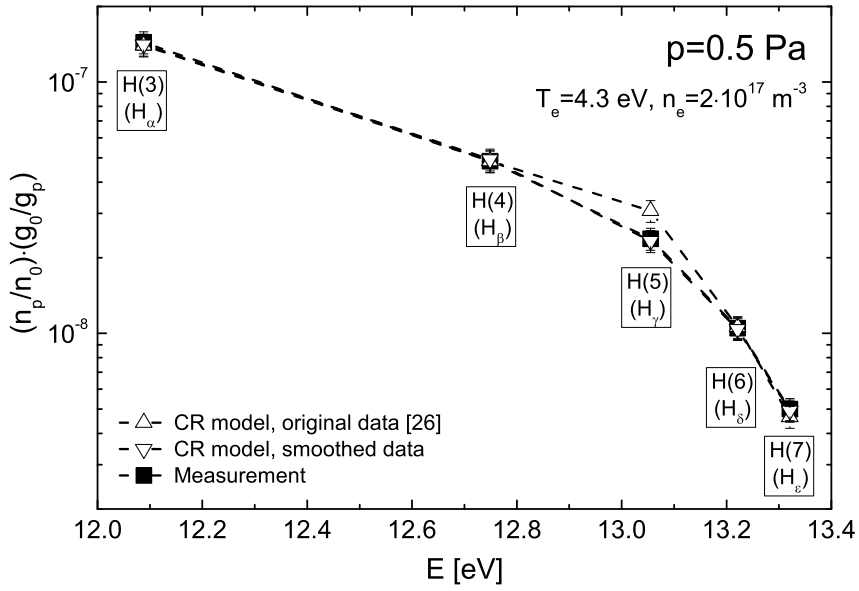

Fig. 5. Boltzmann plot for the hydrogen atom in a mixture of 10% H_2, 5% Ar in He at P=400 W and p=0.5 Pa. Full squares denote the spectroscopic measurement and open triangles the CR model calculations using the original and the smoothed data set.

[38]. The EEDF follows a Maxwellian shape and thus the electron energy distribution can be characterized by a temperature. The absolute value of the electron density ($2 \cdot 10^{17}\,\mathrm{m}^{-3} - 4 \cdot 10^{16}\,\mathrm{m}^{-3}$, depending mainly on the pressure) is determined by means of microwave interferometry and double probe measurements.

The noble gases added to the plasma are used as diagnostic gases to determine the line-of-sight averaged electron temperature: the temperature (4.4 eV − 2.1 eV) is deduced from the intensities of the Ar line at 750 nm and the He line at 728 nm [5,39]. The electron temperatures determined from these two lines are in good agreement. By varying the percentage of the Ar and He admixture it was checked that the influence of the noble gases on the population densities of the hydrogen atom is negligible small.

For these plasma parameters all excitation channels except for the effective excitation from the ground state are of minor importance: the recombination process which couples the excited states of H to H^+ is of no relevance since the ionization degree is low and the electron temperature is higher than 2.0 eV. The efficiency of coupling to H^-, H_2 and H_2^+ depends linearly on the density of these species. Due to the high dissociation degree and the small negative ion density ($n_{H^-}/n_H < 10^{-3}$) these coupling channels also are of no major rel-

evance. Dissociative recombination of H_3^+ populates the state H(2) primarily. Since the probability for stepwise excitation is low due to the small electron density, this coupling channel can be neglected also. However, the relevance of the neglected channels was checked in the second of the iteration steps described in the following.

The Balmer line emissivity measured spectroscopically is compared with results predicted by the CR model using the known plasma parameters. The comparison is performed by means of a Boltzmann plot which allows to compare measurement and calculated results for low and high quantum numbers simultaneously. Figure 5 shows the Boltzmann plot for population densities determined from the first five Balmer lines at p=0.5 Pa.

In the first step CR model calculations for coupling just to the ground state were performed. Electron density and electron temperature are taken from interferometry and He-spectroscopy, respectively. For both input data sets the agreement between measurement and model is very good, with the exception of the level H(5). Using the original data set, for H(5) a obvious deviation between calculation and measurement arises from the discontinuity in the shape of the rate coefficients shown in figure 3. In contrast, the results of the calculation based on the smoothed rate coefficients are in very good agreement with the measured values for all quantum numbers.

In the second step the agreement of measurement and model was optimized by varying n_e and T_e and introducing the other coupling channels. No or only very small variations of n_e and T_e are necessary to minimize the deviation of measured from calculated values. Additionally, only small additions of H^- ($n_{H^-}/n_H \approx 10^{-3}$) and H_2^+ ($n_{H_2^+}/n_H \approx 10^{-3}$) are needed. These deviations are within the error bar of the diagnostics and represent the expected ion densities. The results shown in figure 5 represent the result of this second iteration step. For both spectroscopic measurements and CR model calculations an relative error of 10 % has been estimated.

The six coupling processes described by equation (7) show different dependencies on quantum number, electron temperature and electron density. Varying T_e, n_e or the densities of the six species with quasi-constant density changes the shape of the population densities shown in the Boltzmann plot in different ways. Thus, by applying a validated CR model to spectroscopically determined population densities it is possible to determine one or more unknown plasma parameters. To minimize the experimental expenditure, usually the line ratio method is used, i.e. the calculated ratio of the emission of two Balmer lines is adjusted to the measured ratio. This method was described in [6,18,40] for the determination of the dissociation degree, in [41] for the electron density and in [24] for the density of the negative hydrogen ion.

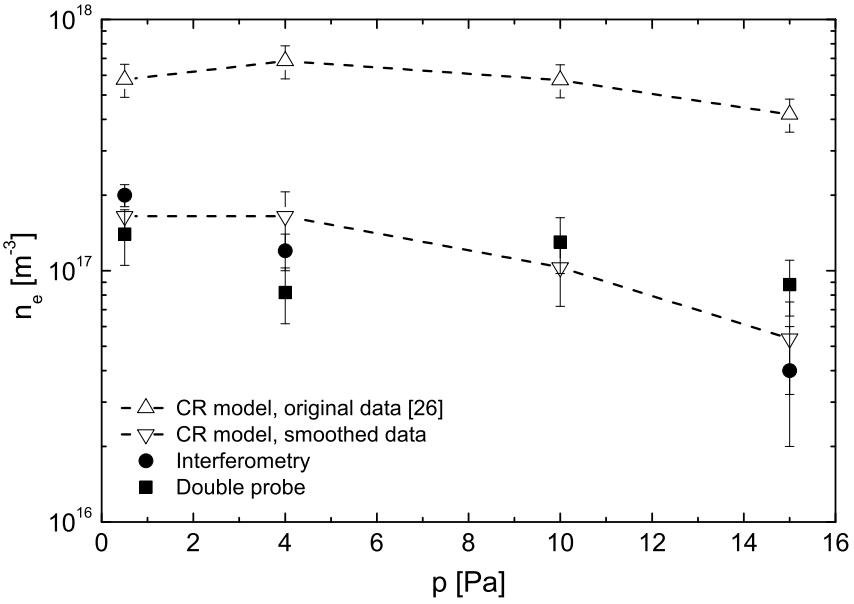

Fig. 6. Electron density determined using the CR model in a mixture of 10% H_2, 5% Ar in He at P=400 W. Full squares denote results of double probe measurements, full circles interferometric results and open triangles the CR model calculations using the original and the smoothed data set.

For further verification of the smoothing procedure the line ratio H_β/H_γ was used to determine the electron density for all pressures. This specific line ratio is used quite often for diagnostic purposes in low pressure, low temperature plasmas since typically the influence of optical thickness and the other excitation channels besides effective excitation is low which reduces the number of free parameters. The smoothing procedure strongly influences results based on the H_β/H_γ line ratio since the upper state of the H_γ transition is H(5). Figure 6 shows a comparison of the electron densities obtained by applying the line ratio method with the values obtained by means of interferometry and double probe measurements.

It can be seen that the results of interferometer and double probe agree well for all pressures. The electron densities resulting from the CR model using the original data set are by a factor of three to ten higher than the results of the two other measurement methods. When the smoothed data set is used, the agreement between the spectroscopically determined electron densities and the results of interferometer and double probe improves significantly.

With increasing pressure the influence of the optical thickness on the line ratio H_β/H_γ increases: while for p=0.5 Pa the calculated ratio is increased by a factor 1.08 compared to the optical thin case, for p=15 Pa the factor

amounts to 1.23. For the interferometric measurements an absolute error of $2 \cdot 10^{16}\,\mathrm{m}^{-3}$ is used which is mainly caused by the phase shift determination. For the densities determined by the double probe a relative error of 25 % is used. The error of the spectroscopic method depends on the electron density: in the range $10^{17}\,\mathrm{m}^{-3} < \mathrm{n_e} < 10^{19}\,\mathrm{m}^{-3}$ the line ratio $\mathrm{H}_\beta/\mathrm{H}_\gamma$ strongly depends on the electron density. For higher and lower electron densities the method becomes more insensitive [24].

6 Conclusion

The flexible package `Yacora` was used to construct a CR model for the hydrogen atom based on the most recent cross sections available in literature. The model incorporates six different excitation channels which can be of relevance in low pressure, low temperature plasmas: effective excitation of H, recombination of H^+, dissociative excitation of H_2, dissociative recombination of H_2^+, dissociative recombination of H_3^+ and mutual neutralization of H^- and H_x^+.

The model was used to interpret Balmer line emissivities measured by OES on an uniform and stationary ECR driven plasma with high dissociation degree and low ionization degree, i.e. electron collision excitation of H is the dominant population channel. For low electron energies a discontinuity appears between the cross sections for the processes $\mathrm{H}(1) \rightarrow \mathrm{H}(5)$ and $\mathrm{H}(1) \rightarrow \mathrm{H}(6)$. This discontinuity is explained by slow convergence of the existing R-Matrix calculations for the main quantum number $q = 5$ and was removed by a smoothing procedure. Since the smoothing procedure is based on rate coefficients, is restricts the applicability of the CR model to plasmas with Maxwellian EEDF.

To check the validity of the smoothing procedure, measured population densities were compared with CR model results based on both the original data set and the smoothed data set. It has been shown by means of a Boltzmann plot that using the smoothed data set produces much better agreement between calculated and experimentally derived population densities.

When the CR model based on the original data is applied to determine the electron density by the $\mathrm{H}_\beta/\mathrm{H}_\gamma$ line ratio method, the results deviate by a factor of three to ten compared with the values obtained by microwave interferometry or a double probe system. When the smoothed data set is used, an almost perfect agreement is obtained.

The described results indicate that for low electron temperatures the rate coefficient for $\mathrm{H}(1) \rightarrow \mathrm{H}(5)$ determined by the performed fit procedure represents measurements much better than the cross sections and rate coefficients available in literature. Thus, to increase the accuracy of the results of plasma

diagnostics basing on the Balmer line radiation of low pressure, low temperature plasmas, the smoothed input data set should be used as long as no more recent data is available.

References

[1] Hippler R, Pfau S, Schmidt M, Schoenbach K. Low Temperature Plasma Physics. Berlin: Wiley-WCH, 2001.

[2] Hutchinson IH. Principles of Plasma Diagnostics. Cambridge: Cambridge University Press, 2002.

[3] Lochte-Holtgreven W. Plasma Diagnostics. Amsterdam: North-Holland Publishing, 1968.

[4] Griem HR. Principles of Plasma Spectroscopy. Cambridge: Cambridge University Press, 1997.

[5] Fantz U. Basics of plasma spectroscopy. Plasma Sources Sci Technol 2006;15:S137-S147.

[6] Von der Gathen VS, Döbele HF. Critical comparison of emission spectroscopic determination of dissociation in hydrogen RF discharges. Plasma Chem Plasma Proc 1996;16:461-486.

[7] Wilson R. The spectroscopy of non-thermal plasmas. J Quant Spectrosc Radiat Transfer 1962;2:477-490.

[8] Bates DR, Kingston AE, McWirter RWP. Recombination between electrons and atomic ions. I. Optically thin plasmas. Proc R Soc Lond A 1962;267:297-312.

[9] Fujimoto T. Kinetics of ionization-recombination of a plasma and population density of excited ions. I. Equilibrium plasma. J Phys Soc Japan 1979;47:265-272.

[10] McWirter RWP, Summers HP. Applied Atomic Collision Physics. New York: Academic, 1984.

[11] Johnson LC, Hinnov E. Ionization, recombination, and population of excited levels in hydrogen plasmas. J Quant Spectrosc Radiat Transfer 1973;13:333-358.

[12] Sawada K, Fujimoto T. Effective ionization and dissociation rate coefficients of molecular hydrogen in plasma. J Appl Phys 1995;78:2913-2924.

[13] Summers HP. The ADAS User Manual, version 2.6 (http://adas.phys.strath.ac.uk).

[14] Schram DC. Plasma processing and chemistry. Pure Appl Chem 2002;74:369-380.

[15] Kraus W, Speth E, Feist JH, Frank P, Heinemann B, Riedl R, Trainham R, Jacquot C. Large-area radio frequency plasma sources for fusion applications. Rev Sci Instrum 1998;69:956-958.

[16] Fantz U, Franzen P, Kraus W, Berger M, Christ-Koch S, Fröschle M, Gutser R, Heinemann B, Martens C, McNeely P, Riedl R, Speth E, Wünderlich D. Negative ion RF sources for ITER NBI: status of the development and recent achievements. Plasma Phys Contr Fus 2007;49:B563-B580.

[17] Greenland PT. Collisional-radiative models with molecules. Proc Roy Soc Lond A 2001;457:1821-1839.

[18] Behringer K, Fantz U. The influence of opacity on hydrogen excited-state population and applications to low-temperature plasmas. New J Phys 2000;2:23.1-23.19.

[19] Vlček J, Pelikán V. Excited level populations of argon atoms in a non-isothermal plasma. J Phys D 1986;19:1879-1888.

[20] Otorbaev DK, Buuron AJM, Guerassimov NT, van de Sanden MCM, Schram DC. Spectroscopic measurement of atomic hydrogen level populations and hydrogen dissociation degree in expanding cascaded arc plasmas. J Appl Phys 1994;76:4499-4510.

[21] Butcher J. A history of Runge-Kutta methods. Appl Num Math 1996;20:247-260.

[22] Cohen CD, Hindmarsh AC. CVODE, a stiff/nonstiff ODE solver in C. Computers in Physics 1996;10:138-143.

[23] Godyak VA. Nonequilibrium EEDF in gas discharge plasmas. IEEE Trans Plas Sci 2006;34:755-766.

[24] Fantz U, Wünderlich D. A novel diagnostic technique for $H^-(D^-)$ densities in negative hydrogen ion sources. New J Phys 2006;8:301.1-301.23.

[25] Florescu-Mitchell AI, Mitchell JBA. Dissociative recombination. Physics Reports 2006;430:277-374.

[26] Janev RK, Reiter D, Samm U. Report, Jül–4105. Forschungszentrum Jülich, Jülich, 2003.

[27] Kulander FC, Guest MF. Excited electronic states of H_3 and their role in the dissociative recombination of H_3^+. J Phys B 1979;12:L501-L504.

[28] Datz S, Sundström G, Biedermann C, Broström L, Danared H, Mannervik S, Mowat JR, Larsson M. Branching Processes in the Dissociative Recombination of H_3^+. Phys Rev Lett 1995;74:896-899.

[29] Johnson CE. Lifetime of the $c\,^3\Pi_u$ metastable state of H_2, D_2, and HD. Phys Rev A 1972;5:1026-1030.

[30] Eerden MJJ, van de Sanden MCM, Otorbaev DK, Schram DC. Cross section for the mutual neutralization reaction $H_2^+ + H^-$, calculated in a multiple-crossing Landau-Zener approximation. Phys Rev A 1995;51:3362-3365.

[31] Johnson LC. Approximations for collisional and radiative transition rates in atomic hydrogen. Astrophys J 1972;174:227-236.

[32] Witthoeft M, Colgan J, Pindzola MS, Ballance CP, Griffin DC. Electron-impact excitation of Li to high principal quantum numbers. Phys Rev A 2003;68:022711.1-022711.6.

[33] Anderson H, Ballance CP, Badnell NR, Summers HP. An R-matrix with pseudostates approach to the electron-impact excitation of H I for diagnostic applications in fusion plasmas. J Phys B 2000;33:1255-1262.

[34] Ballance CP. Private communication (2007).

[35] Janev RK, Smith JJ. Atomic and Plasma–Material Interaction Data for Fusion 4. Wien:IAEA, 1993.

[36] Geller R. Electron Cyclotron Resonance Ion Sources and ECR Plasmas. Bristol and Philadelphia: Institute of Physics Publishing, 1996.

[37] Popov OA. High Density Plasma Sources: Design, Physics, and Performance. New York: Noyes Publications, 1996.

[38] Dietrich S. Verifikation von optischen Diagnostikmethoden an H_2/D_2-Plasmen zur Entwicklung einer Standardmethode für negative Ionenquellen. Ph.D. thesis, Universität Augsburg, Augsburg, 2008.

[39] Donnelly VM. Plasma electron temperatures and electron energy distributions measured by trace rare gases optical emission spectroscopy. J Phys D 2004;37:R217-R236.

[40] Fantz U. Emission spectroscopy of molecular low pressure plasmas. Contrib Plas Phys 2004;44:508-515.

[41] Sawada K, Eriguchi K, Fujimoto T. Hydrogen-atom spectroscopy of the ionizing plasma containing molecular hydrogen: line intensities and ionization rate. J Appl Phys 1993;73:8122-8125.